Spectrum Sensing for Cognitive Radio Networks Based on Blind Source Separation

Siavash Sadeghi Ivrigh, Seyed Mohammad-Sajad Sadough
Cognitive Telecommunication Research Group,
Department of Electrical Engineering,
Faculty of Electrical and Computer Engineering,
Shahid Beheshti University G.C., 1983963113, Tehran, IRAN
si.sadeghi@mail.sbu.ac.ir, s_sadough@sbu.ac.ir

Received April 24, 2012; revised October 9, 2012; accepted November 2, 2012; published April 30, 2013

Abstract

Cognitive radio (CR) is proposed as a key solution to improve spectral efficiency and overcome the spectrum scarcity. Spectrum sensing is an important task in each CR system with the aim of identifying the spectrum holes and using them for secondary user's (SU) communications. Several conventional methods for spectrum sensing have been proposed such as energy detection, matched filter detection, etc. However, the main limitation of these classical methods is that the CR network is not able to communicate with its own base station during the spectrum sensing period and thus a fraction of the available primary frame cannot be exploited for data transmission. The other limitation in conventional methods is that the SU data frames should be synchronized with the primary network data frames. To overcome the above limitations, here, we propose a spectrum sensing technique based on blind source separation (BSS) that does not need time synchronization between the primary network and the CR. Moreover, by using the proposed technique, the SU can maintain its transmission with the base station even during spectrum sensing and thus higher rates are achieved by the CR network. Simulation results indicate that the proposed method outperforms the accuracy of conventional BSS-based spectrum sensing techniques.

Keywords: Cognitive radio, spectrum sensing, blind source separation techniques, Kurtosis metric.

The material in this paper was presented *in part* at the International eConference on Computer and Knowledge Engineering (ICCKE), Mashahd, Iran, October 2011.

http://dx.doi.org/10.3837/tiis.2013.04.001

1. Introduction

In cognitive radio (CR) systems [1], spectrum sensing is a fundamental block for deciding if the primary user (PU) is in operation or not. If the spectrum sensing block announces that the PU is not in operation, the secondary user (SU) starts utilizing the vacant frequency band and transmits its data over that frequency band, opportunistically [2]. There are different methods proposed for spectrum sensing in the literature such as energy detection (ED) [3] [4] [5] [6], cyclostationary detection and matched filter detection as propose in [7], for instance. In the ED method, the received signal energy is measured and compared to a threshold to make a decision on the presence/absence of the PU over the desired channel. Cyclostationary spectrum sensing uses the statistical properties of signal and noise to detect the presence of the PU [7]. If the transmitted PU signal is known, matched filtering is the optimal method for detecting the activity of the PU. In this approach, the CR should demodulate the received signal; therefore, it requires some PU signaling features such as bandwidth, carrier frequency and modulation type [7].

Conventional spectrum sensing have two main limitations as described below. The first limitation is that the CR should not be in operation during the spectrum sensing period. This is due to the fact that conventional spectrum sensing techniques are not able to differentiate between primary and cognitive signals and the CR signal would certainly impose an interference on the primary network. The second limitation is the requirement of perfect synchronization between primary and cognitive frames. More precisely, spectrum sensing is performed at the beginning of the PU data frame, while the CR transmitter is not in operation during this time. If the spectrum sensing decision is in favor of the absence of the PU, then the CR is allowed to transmit over the rest of the PU frame and this forces the CR network to be synchronized with PU frames. Obviously, the above limitation reduces the throughput of the CR network due to the time dedicated to spectrum sensing.

Blind source separation (BSS) techniques [8] are recently suggested for spectrum sensing in CR systems [8]. The advantage of BSS spectrum sensing is that the CR can maintain its transmission even during the spectrum sensing process. Obviously, this is related to the ability of BSS techniques to differentiate signals from a mixture of signals. Consequently, higher rates can be achieved by the secondary network. Besides, by using BSS, the secondary network does not necessarily require to know the beginning of the PU data frame in order to force the CR to be inactive and then start the spectrum sensing process. Thus, the secondary network can start sensing the PU activity at any time within the primary frame and this relaxes the requirement of synchronization between the PU and CR transmitted frames. In [10], BSS is used to separate the mixture of signals with different frequency bands. In [11], a BSS-based spectrum sensing is applied to separates sensed signals and then with respect to the correlation between separated signals, a decision is made about the absence or presence of the PU. In [12], BSS is used to estimate the noise variance and to implement blind spectrum sensing. In [13], a BSS-spectrum sensing based on independent component analysis (ICA) algorithm is used to separate sensed signals and then Kurtosis is used to indicate the statistical properties of separated signals. In [14] a novel framework for spectrum sensing is proposed that combines BSS spectrum sensing and covariance based spectrum sensing. In [15], the authors have proposed a BSS-based spectrum sensing but this work does not consider the practical scenario where the PU activity has a dynamic ON/OFF switching. ICA method mesures the negentropy

metric of observed signals to seprate the signals, but Kurtosis metric uses the fourth comulant of observed signal to separate them.

In this paper, we provide a more in depth and complete analysis of our BSS-based spectrum sensing compared to our initial contribution [13] that was only based on the ICA algorithm. Our aim consists in comparing different widely-adopted BSS techniques and algorithms in context of spectrum sensing and finding the technique leading to the most accurate BSS-based spectrum sensing technique. We focus on the family of Kurtosis methods for separating the sensed signals and determining the properties of the separated signals in order to make a decision about the presence or absence of the PU. We provide simulation results in the context of CR, to analyze the performance achieved by using the Kurtosis metric in comparison to the Negentropy metric that is usually adopted in BSS. In addition, here we propose a dynamic algorithm for CR transmitter to transmit its data in dynamic senario. As we will see in Section 3.2, in the dynamic senario the sensed state of PU in the previous sensing frame determines the CR transmitter activity in the current sensing frame. More precisely, the decision about the presence or absence of the PU in the $(n-1)$-th frame, affects the transmission or not of the CR user in the n-th sensing frame. In fact, we have adopted a methodology in which there are some sort of dependency (memory) to the previous frame's decision in the spectrum sensing process, that is modeled by a Markov process. As we will see in simulation results, if the state of PU in previeous sensing frame, is repeated in the current sensing frame with high probability, the performance of the proposed method would be better. This feature constitutes the main contribution of our paper since in conventional spectrum sensing methods, the performance is independent from the activity model of the PU.

The rest of this paper is organized as follows. Spectrum sensing problem formulation and the assumed system model are presented in Section 2. In Section 3, we give a short description of conventional BSS methods proposed for spectrum sensing and then explain our proposed methodology. Section 4 provides simulation results and discussions, and finally Section 5 draws our conclusions.

2. Spectrum Sensing System Model

The objective of spectrum sensing in a CR network is to monitor the activity of the primary network; i.e., to indicate the presence or absence of the PU. Sensing the presence of PU over a specific frequency band is usually viewed as a binary hypothesis testing as:

$$\begin{cases} \mathrm{H}_0: & \text{PU is not in operation,} \\ \mathrm{H}_1: & \text{PU is in operation.} \end{cases} \tag{1}$$

In the above binary hypothesis, as errors may happen during the sensing process, the real state of the PU and the sensed (estimated) state of the PU are not necessarily the same. We denote the real state of the PU by H_i^{PU} ($i=0$ means that the PU is not in operation and $i=1$ means that the PU is in operation) and denote the sensed state of the PU by H_i^{CN} ($i=0$ it means that the PU is sensed as absent and $i=1$ means that the PU is sensed as present). Thus, two different types of errors, referred to as miss detection and false alarm, can be defined. The probabilities of these errors are defined as:

$$P_m = P(\mathrm{H}_0^{CN} \mid \mathrm{H}_1^{PU}), \tag{2}$$

and

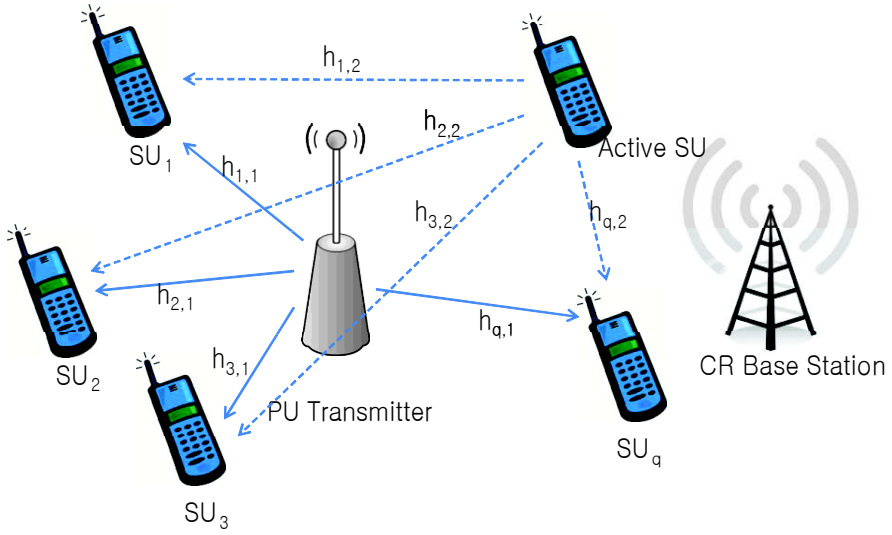

Fig. 1. Considered system model with q SUs, one PU transmitter and one active SU transmitter.

$$P_f = P(\mathrm{H}_1^{CN} \mid \mathrm{H}_0^{PU}), \tag{3}$$

respectively. Obviously, an accurate spectrum sensing method is characterized by low values for P_f and P_m probabilities.

The considered system architecture is illustrated in **Fig. 1**. In this network, the CR base station operates as a fusion center for cooperative spectrum sensing. When the spectrum sensing fusion center indicates the absence of PU, one of the SUs in CR network is allowed to send its data, and other SUs continue to sense the channel. The received signal at the j-th SU which is in general the superposition of the PU and the active SU signals, can be written as:

$$\mathbf{y}_j = h_{j,1}\mathbf{a}^{PN} + h_{j,2}\mathbf{a}^{CN} + \mathbf{n}_j, \tag{4}$$

where $\mathbf{a}^{PN} = [a_1^{PN}, a_2^{PN}, \ldots, a_L^{PN}]$ is the vector containing L symbols (L is the sensing frame length) transmitted by the PU, $\mathbf{a}^{CN} = [a_1^{CN}, a_2^{CN}, \ldots, a_L^{CN}]$ is the vector containing L symbols transmitted by the active SU (simultaneously with the PU symbols), and $\mathbf{n}_j = [n_{j,1}, n_{j,2}, \ldots, n_{j,L}]$ is the Gaussian complex noise vector distributed as $\mathbf{n}_j : \mathbb{CN}(\mathbf{0}, \sigma_{n_j}^2 \mathbf{I}_L)$ with $\mathbf{I}_L$ being the $L \times L$ identity matrix. Moreover, $h_{j,1}$ is the Rayleigh distributed channel between the PU and the j-th SU and $h_{j,2}$ is the channel between the active SU and the j-th SU with Rayleigh distribution too.

When the SU is in operation, depending on the two hypothesis H_0^{PN} and H_1^{PN} characterizing the activity pf the PU, we have:

$$\mathbf{y}_j = \begin{cases} h_{j,2}\mathbf{a}^{CN} + \mathbf{n}_j & \mathrm{H}_0^{PN} \\ h_{j,1}\mathbf{a}^{PN} + h_{j,2}\mathbf{a}^{CN} + \mathbf{n}_j. & \mathrm{H}_1^{PN} \end{cases} \tag{5}$$

Similarly, when the SU is not in operation, we have:

$$\mathbf{y}_j = \begin{cases} \mathbf{n}_j & \mathrm{H}_0^{PN} \\ h_{j,1}\mathbf{a}^{PN} + \mathbf{n}_j. & \mathrm{H}_1^{PN} \end{cases} \tag{6}$$

Let us denote the number of SUs by q. For convenience, we rewrite Equations 4 in matrix form as:

$$\mathbf{Y} = \mathbf{HA} + \mathbf{N} \tag{7}$$

where

$$\mathbf{Y} = \begin{bmatrix} y_{1,1} & y_{1,2} & \cdots & y_{1,L} \\ y_{2,1} & y_{2,2} & \cdots & y_{2,L} \\ \vdots & \vdots & \ddots & \vdots \\ y_{q,1} & y_{q,2} & \cdots & y_{q,L} \end{bmatrix} = \begin{bmatrix} \mathbf{y}_1 \\ \mathbf{y}_2 \\ \vdots \\ \mathbf{y}_q \end{bmatrix} \tag{8}$$

where $y_{q,l}$ is the l-th observed symbol by the q-th SU, and

$$\mathbf{A} = \begin{bmatrix} \mathbf{a}^{PU} \\ \mathbf{a}^{CR} \end{bmatrix} = \begin{bmatrix} \mathbf{a}_1 \\ \mathbf{a}_2 \end{bmatrix} \tag{9}$$

and

$$\mathbf{H} = \begin{bmatrix} h_{11} & h_{12} \\ \vdots & \vdots \\ h_{q1} & h_{q2} \end{bmatrix} \tag{10}$$

where h_{ij} is the channel coefficient between SUs and the PU, and

$$\mathbf{N} = \begin{bmatrix} n_{1,1} & n_{1,2} & \cdots & n_{1,L} \\ n_{2,1} & n_{2,2} & \cdots & n_{2,L} \\ \vdots & \vdots & \ddots & \vdots \\ n_{q,1} & n_{q,2} & \cdots & n_{q,L} \end{bmatrix} = \begin{bmatrix} \mathbf{n}_1 \\ \mathbf{n}_2 \\ \vdots \\ \mathbf{n}_q \end{bmatrix} \tag{11}$$

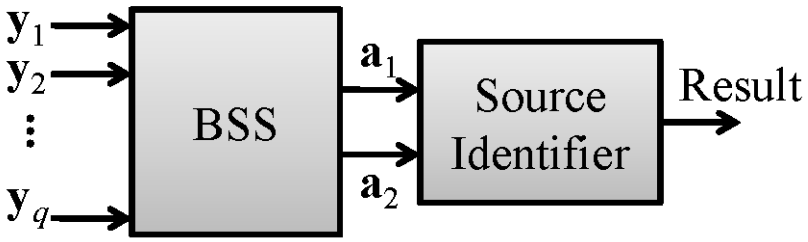

Fig. 2. The block diagram of proposed spectrum sensing method.

3. Spectrum sensing methodology based on BSS

In this Section, we aim at explaining the BSS-based spectrum sensing methodology that we have adopted in this paper. As shown in **Fig. 2**, our BSS-based spectrum sensing is composed of two subblocks. The first subblock denoted as BSS in **Fig. 2**, separates the mixture of two signals and provides at its output the two separated components. However, it is not clear at the output of this block that each component is the primary signal, the CR signal or the ambient noise. The second block denoted as *source identifier*, is used in order to recognize each separated component. In what follows, we provide more details about the functionality of each subblock and in this way we explain the proposed methodology for spectrum sensing.

3.1 Blind source separation

In BSS problems, we have several independent source signals for which we have not any information about the power and other parameters. Also, we do not dispose of any information about the channel between the sources and the sensors. Obviously, we just dispose of some sensors' observations. Each observation is a linear combination of all independent sources. Starting from the matrix form of our system model 7, we have:

$$\mathbf{Y} = \mathbf{HA} + \mathbf{N}, \tag{12}$$

where $\mathbf{Y}$ is our observation which is the linear combination of independent sources gathered in matrix $\mathbf{A}$ and $\mathbf{H}$ is the linear transformation matrix (in our scenario $\mathbf{H}$ is the channel matrix) and $\mathbf{N}$ is the Gaussian noise. According to the general methodology adopted in BSS, to estimate the source signals, we first have to estimate $\mathbf{H}$ and then we multiply our observation vector $\mathbf{Y}$ by the inverse of $\mathbf{H}$. Different algorithms are proposed in the literature for estimating the linear transformation matrix $\mathbf{H}$ such as Independent Component Analysis (ICA) [16], Multiuser Kurtosis algorithm (MUK) [17], Trilinear Alternating Least Squares (TALS) and improved version of that called comfac [18][19], TFBSS (Blind Source Separation Using Time Frequency Distributions) [20] for instance. In this paper, we aim at comparing the performance achieved by each of the above methods in order to identify the method leading to the the more accurate spectrum sensing in the context of CR systems. In Equation 12, without considering the noise for the moment we get:

$$\mathbf{Y} = \mathbf{HA} \tag{13}$$

After some preprocessing (centering and whitening) of data, by multiplying the observation matrix by the equalization matrix $\mathbf{W}$, we get:

$$\mathbf{Z} = \mathbf{WY} = \mathbf{W}(\mathbf{HA}) = (\mathbf{WH})\mathbf{A} \tag{14}$$

The ideal case for equalization is when $\mathbf{WH} = \mathbf{I}$ where $\mathbf{I}$ is the identity matrix. There are several algorithms to estimate the matrix $\mathbf{W}$ of size $2 \times q$. The general solution to find the matrix $\mathbf{W}$ is to define a cost function for matrix $\mathbf{Z}$ and try to minimize (or maximize) the defined cost function. Each defined cost function and the way to maximize (or minimize) leads to a different BSS method. Defining the cost function is based on our assumption about the independent sources. For example, the main assumption for sources could be their non-Gaussianity.

Independent component analysis (ICA) uses the Negentropy metric to measure the non-Gaussian property of the source signal [8]. Negentropy is based on the information theoretic quantity of (differential) entropy. Let us define $\mathbf{w}_i$ as the i-th row of matrix $\mathbf{W}$. Then the entropy of random vector $\mathbf{w}_i\mathbf{Y}$ with each entry being identically distributed following the probability density function (pdf) $p_i(\eta)$ defined as:

$$Entropy(\mathbf{w}_i\mathbf{Y}) = -\int p_i(\eta)\log(p_i(\eta))d\eta. \tag{15}$$

Entropy shows the unpredictability of a random variable; the more random or unpredictable a random variable, the larger entropy it has. It could be shown that in all of the random variables with unit variance, Gaussian random variable has the most entropy. So we define Negentropy as:

$$J(\mathbf{w}_i\mathbf{Y}) = Entropy(y_{gauss}) - Entropy(\mathbf{w}_i\mathbf{Y}) \tag{16}$$

where y_{gauss} is a Gaussian random variable with the same covariance matrix with $\mathbf{w}_i\mathbf{Y}$. Negentropy is always positive, and it is zero if and only if $\mathbf{w}_i\mathbf{Y}$ has a Gaussian distribution. Negentropy is a suitable way for measuring the non-Gaussian property, but it is difficult to compute, therefore the approximation of the Negentropy is usually used. It can be shown that one of the approximations of Negentropy is [21] [8]:

$$J(\mathbf{w}_i\mathbf{Y}) \propto [E\{G(\mathbf{w}_i\mathbf{Y})\} - E\{G(\nu)\}]^2 \tag{17}$$

where $G(.)$ is a non-quadratic function and ν is a given random variable with zero mean and unit variance. The following choices for $G(.)$ are usually adopted in the literature:

$$G_1(u) = \frac{1}{a_1}\log\cosh a_1 u,\ G_2(u) = -\exp(-u^2/2) \tag{18}$$

where $1 \le a_1 \le 2$ is a constant and in this paper, we have used the function G_2.

We now explain the methodology of the fast-ICA algorithm to estimate the i-th row in matrix $\mathbf{W}$, i.e., the vector $\mathbf{w}_i$ which is denoted as one of the independent components. We first assign a random value to vector $\mathbf{w}_i$ and then update the value with a learning rule. In fact fast-ICA is a fixed-point iterative algorithm that finds the maxima of non-Gaussianity of $\mathbf{w}_i\mathbf{Y}$ as measured in (17). The derivation of the function $G_2(u)$ that we have adopted is obtained as:

$$g'(u) = u\exp(-u^2/2). \tag{19}$$

The methodology for source separation used in the fast-ICA algorithm is as follows:

1. For $i = 1\text{to}\,2$
2. Choose an initial weight vector $\mathbf{w}_i$
3. Let $\mathbf{w}_i^T = E[\mathbf{Y}g(\mathbf{w}_i\mathbf{Y})] - E[g'(\mathbf{w}_i\mathbf{Y})]\mathbf{w}_i^T$
4. Let $\mathbf{w}_i^T = \mathbf{w}_i^T / \mathbb{P}\mathbf{w}_i^T\,\mathbb{P}$
5. If not converged, go to 3.
6. End for

In this paper, we mainly focus to maximize the Kurtosis metric for separating the mixed signals. In this method, Kurtosis metric helps us measure the non-Gaussian property of the separated signals.

After preprocessing (centering and whitening), the observed vector signal, $\mathbf{Y}$ is filtered by $2\times q$ matrix equalizer $\mathbf{W}$ that produces the 2×1 vector output $\mathbf{Z} = [\mathbf{z}_1, \mathbf{z}_2]^T$. This operation can mathematically represents as:

$$\mathbf{Z} = \mathbf{WY} = \mathbf{WHA} + \mathbf{n}' = \mathbf{GA} + \mathbf{n}' \tag{20}$$

where $\mathbf{G} = \mathbf{WH}$ is the 2×2 global response matrix, and $\mathbf{n}' = \mathbf{WN}$ is the colored noise at the receiver output. The receiver (BSS block) outputs $\mathbf{z}_j, j = 1,2$ should ideally match the transmitted signals $\mathbf{a}_j, j = 1,2$ [21] [17].

We define:

$$K_{a_j} = \text{Kurtosis}[\mathbf{a}_j] = K[\mathbf{a}_j] \tag{21}$$

$$\sigma_a^2 = E[|\,\mathbf{a}_j\,|^2], j = 1,2 \tag{22}$$

where:

$$K[x] = E[|\,x^4\,|] - 2E^2[|\,x\,|^2] - |\,E(x^2)\,|^2 \tag{23}$$

It can be proved [17] that:

$$E[|\,\mathbf{z}_j\,|^2] = \sigma_a^2 \sum_{l=1}^{2} |\,g_{jl}\,|^2, j = 1,2 \tag{24}$$

$$K(\mathbf{z}_j) = \sum_{l=1}^{2} K_{a_l} |\,g_{jl}\,|^4, j = 1,2 \tag{25}$$

where, g_{jl} is the element in the j-th row and l-th column of matrix $\mathbf{G}$.

In can be proofed [17] that the following set of conditions is necessary and sufficient for blind recovery of the transmitted signals.

$$\begin{aligned} &C1: |K(z_j(k))| = |K_{a_j}|, j = 1,2 \\ &C2: E\,|z_j(k)|^2 = \sigma_{a_j}^2, j = 1,2 \\ &C3: E(z_l(k) z_j^*(k)) = 0, l \neq j \end{aligned} \tag{26}$$

The above conditions for BSS problem leads to solving the following optimization problem [17]:

$$\begin{cases} \max\limits_{\mathbf{G}} F(\mathbf{G}) = \sum\limits_{j=1}^{2} |K(\mathbf{z}_j)| \\ \text{subject to: } \mathbf{G}^H \mathbf{G} = \mathbf{I}_2 \end{cases} \tag{27}$$

It can be proved that the maximum of each absolute value in above optimization is equal to recovering each independent source [21]. In fact the MUK algorithm separates signals in a way that the separated signals have the maximum possible value of Kurtosis metric, where the separated signals have unit variance. Kurtosis metric for Gaussian random variable is equal to zero and for non-Gaussian random variable is non-zero. In other words, the random variable with more unpredictable property has lower Kurtosis value. This feature is exploited in the next Section for identifying different sources, as explained below.

3.2 Spectrum Sensing Based on BSS Algorithm

As explained previously, in the MUK algorithm, the following metric is maximized:

$$F(\mathbf{G}) = \sum_{j=1}^{2} |K(\mathbf{z}_j)| = |K(\mathbf{z}_1)| + |K(\mathbf{z}_2)|. \tag{28}$$

Actually, our spectrum method is based on solving the optimization problem (27). More precisely, solving (27) lets us to recover original signals which is equivalent to performing spectrum sensing, and this process requires the values K_{a_1} and K_{a_2} to be non-zero. This is achieved when the distribution of unknown original signals is non-Gaussian. This requirement is likely to be available in our scenario due to the limited size of vector $\mathbf{z}_j, j = 1,2$ and thus the optimization problem (27) has a solution. Based on the solution obtained for $|K(\mathbf{z}_1)|$ and $|K(\mathbf{z}_2)|$ as a result of the optimization problem (27), we can distinguish how many signal components are present in the considered network and then we can identify the absence or presence of the primary signal, as explained below in more details.

Since (28) is the sum of two absolute values, maximizing it is equivalent to the maximization of each absolute value, individually. We have assumed two independent signals in the channel, therefore the maximum value for these two absolute values in ideal situations will be equal to K_{a_1} and K_{a_2}. As shown in **Fig. 3**, if we have only one independent signal in the channel, only one of these absolute values will take the maximum value (in ideal situations

equal to K_a) and the other one will not have a meaningful maximum. However, when two independent signals are present in the channel, there is a meaningful maximum at the diagrams of $|K(\mathbf{z}_1)|$ and $|K(\mathbf{z}_2)|$. The number of meaningful maximums in diagrams of the absolute values of $|K(\mathbf{z}_1)|$ and $|K(\mathbf{z}_2)|$ is the same as the number of independent signals in the channel (see **Fig. 3**).

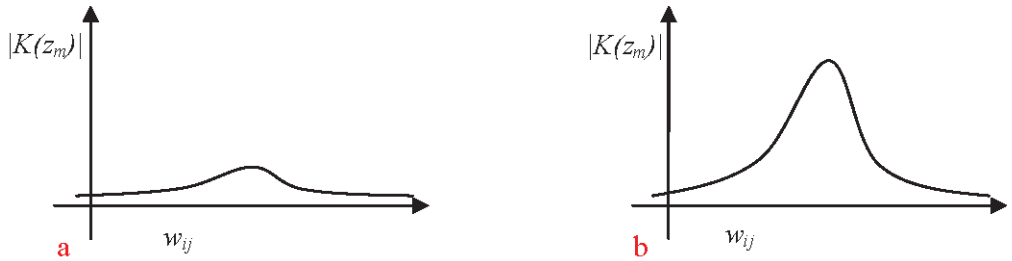

Fig. 3. Kurtosis versus the (i, j)-th element of matrix w. a: There is no source signal in the channel and we observe that the Kurtosis does not have a meaningful maximum value. b: There is an independent source signal in the channel and we observe that the Kurtosis curve has a meaningful maximum.

In MUK method, for separating independent signals, it is desired to find the maximum of $|K(\mathbf{z}_1)|$ and $|K(\mathbf{z}_2)|$ for all $w_{11},\ldots,w_{q1}$ and $w_{12},\ldots,w_{q2}$, respectively. Now if there is no signal present in the channel, in ideal situations, the maximum of the absolute value of both $|K(\mathbf{z}_1)|$ and $|K(\mathbf{z}_2)|$ are equal to zero. However, as stated above, in real scenarios, these absolute values are not exactly equal to zero and have some fluctuations as shown in **Fig. 3a** and the maximum in this case is not meaningful. When there is one signal present in the channel, only the corresponding $|K(\mathbf{z}_i)|(i=1,2)$ would have a meaningful maximum value. Now, if there are two independent signals present in the channel, then both absolute values of $|K(\mathbf{z}_1)|$ and $|K(\mathbf{z}_2)|$ would take a meaningful maximum, which in ideal situations is equal to K_{a_1} and K_{a_2}. By comparing the maximum of the curves with a threshold, it can be decided that the maximum is meaningful or not. Finally the second subblock shown in **Fig. 2**, measures the Kurtosis of separated signals (that is the maximum of the aforementioned absolute values) and make a decision about the presence or absence of the PU. The following steps summarize our adopted spectrum sensing methodology that is adopted at the CR terminal: by using the following rules:

1. When one of the SUs is in operation and transmitting its signal,
   - If the channel sensing part (the source identifier subblock) indicates that two independent signals are present in the channel, then we can conclude that the PU is in operation.
   - If the channel sensing part (the source identifier subblock) indicates that one independent signal is present in the channel, then we can conclude that the PU is NOT in operation.
2. When the SU is NOT in operation,
   - If the channel sensing part (the source identifier subblock) indicates one independent signal in channel, then we can conclude that the PU is in operation.
   - If the channel sensing part (the source identifier subblock) indicates that there are no independent signals present in the channel, then we can conclude that

the PU is NOT in operation.

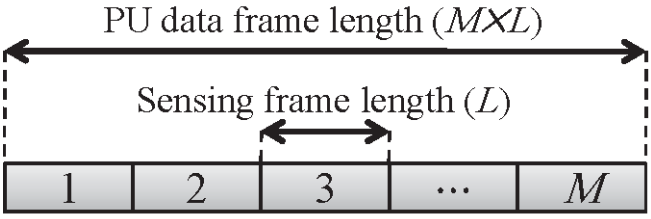

Fig. 4. PU data frame length and the sensing frame length

As shown in **Fig. 4**, the spectrum sensing frame length is smaller than the PU data frame length. More precisely, here we assume that the PU data frame length is equal to $M \times L$ where L is the sensing frame length. The activity of the CR transmitter in a current sensing frame is based on the decision that is made in the previous sensing frame. If the spectrum sensing stated the absence of PU in the current sensing frame, then the CR transmitter would be active in the next sensing frame and if the spectrum sensing finds the PU active, then the CR transmitter would be inactive in the next sensing frame. Thus, our considered BSS-based spectrum sensing is a dynamic system. To study the performance of such a dynamic system, we usually define probabilities P_m and P_f as the probability of miss detection and the probability of false alarm when the CR transmitter is not in operation during the spectrum sensing. Similarly, we define probabilities $\tilde{P}_m$ and $\tilde{P}_f$ as probability of miss detection and probability of false alarm when the CR transmitter is in operation during the spectrum sensing process. Depending on the actual presence or absence of the PU (characterized by hypotheses H_0^{PN} and H_1^{PN} defined previously), and the estimate about this presence or absence made by the CR device (characterized by hypotheses H_0^{CN} and H_1^{CN} defined previously), we can model the dynamic BSS spectrum sensing by a 4-state Markov model with the following states [22] [14]:

- State 1 (S_1): corresponds to the simultaneous occurrence of hypothesis H_1^{CN} and H_0^{PU} (which characterizes a false alarm event),
- State 2 (S_2): corresponds to the simultaneous occurrence of hypothesis H_0^{CN} , H_0^{PU} (i.e., the spectrum sensing decision is correct),
- State 3 (S_3): corresponds to the simultaneous occurrence of hypothesis H_0^{CN} and H_1^{PU} (which characterizes the miss detection event),
- State 4 (S_4): corresponds to the simultaneous occurrence of hypothesis H_1^{CN} and H_1^{PU} (i.e., the spectrum sensing decision is correct).

Markov modeling is usually characterized by a transition probability matrix that in our scenario is a 4×4 matrix denoted $\mathbf{P}$. The (i, j) element of the transition matrix $\mathbf{P}$ is denoted p_{ij} and defined as:

$$p_{ij} = P\{\mathrm{S}_j(n) \mid \mathrm{S}_i(n-1)\} \tag{29}$$

where n represents the n-th time index for the sensing frame. Each element p_{ij} can be calculated easily. For instance, the element p_{11} is obtained as:

$$p_{11} = P\{\mathrm{H}_1^{CN}(n), \mathrm{H}_0^{PU}(n) \mid \mathrm{H}_1^{CN}(n-1), \mathrm{H}_0^{PU}(n-1)\}. \tag{30}$$

Equation (30) can be written as:

$$\begin{aligned} p_{11} &= P\{\mathrm{H}_1^{CN}(n) \mid \mathrm{H}_0^{PN}(n), \mathrm{H}_1^{CN}(n-1), \mathrm{H}_0^{PN}(n-1)\} \\ &\times P\{\mathrm{H}_0^{PN}(n) \mid \mathrm{H}_1^{CN}(n-1), \mathrm{H}_0^{PN}(n-1)\} \end{aligned} \tag{31}$$

Here, we assume that in a given frame, the CR network, has no knowledge about the presence/absence of the PU in the previous sensing frame. So, we have:

$$\begin{aligned} &P\{\mathrm{H}_0^{PN}(n) \mid \mathrm{H}_1^{CN}(n-1), \mathrm{H}_0^{PN}(n-1)\} = \\ &P\{\mathrm{H}_0^{PN}(n) \mid \mathrm{H}_0^{PN}(n-1)\} = q_{00} \end{aligned} \tag{32}$$

where q_{ij} is the transition probability of PU from state i to state j where, $i, j \in \{0,1\}$. As stated above, the decision made by spectrum sensing in the n-th sensing frame depends only on the decision made in the $(n-1)$-th sensing frame and not on the real state of the PU in $(n-1)$-th sensing frame. So, we can rewrite (32) as:

$$p_{11} = q_{00} \times P\{\mathrm{H}_1^{CN}(n) \mid \mathrm{H}_0^{PN}(n), \mathrm{H}_1^{CN}(n-1)\}. \tag{33}$$

As we will see in simulation results, the performance of spectrum sensing with active CR transmitter ($\tilde{P}_m, \tilde{P}_f$) is a little lower than the performance of spectrum sensing with inactive CR transmitter (P_m, P_f). In fact, the CR transmitter affects the performance of spectrum sensing to some extent. More precisely, if the spectrum sensing indicates the presence of the PU, the CR transmitter would be inactive and the decision in the n-th sensing frame would be taken with an active CR transmitter. So Equation (33) can be written as:

$$p_{11} = q_{00} \times P\{\mathrm{H}_1^{CN}(n) \mid \mathrm{H}_0^{PN}(n)\} = q_{00} \times P_f \tag{34}$$

Likewise for p_{22} we would have:

$$p_{22} = q_{00} \times (1 - \tilde{P}_f). \tag{35}$$

All elements of matrix $\mathbf{P}$ can be calculated, in a similar way. To compute the probability of miss detection and probability of false alarm, for dynamic spectrum sensing we should find the probability of state S_3 and S_1 in the mentioned Markov model. To calculate these probabilities, we should find the stationary distribution of the Markov model [22]. We denote by $\pi(n) = [\pi_1(n), \ldots, \pi_4(n)]^T$ the vector of state probabilities at the n-th sensing frame, where $\pi_i(n)$ for $i \in \{1,2,3,4\}$ is the probability of being in the i-th state at the n-th sensing frame, i.e., $\pi_i(n) = P\{\mathrm{S}_i(n)\}$. In the Markov model we have [22]:

$$\pi(n) = \mathbf{P}^n \times \pi(0). \tag{36}$$

To compute the stationary distribution of Markov model we have [22]:

$$\pi = \lim_{n\to\infty}\pi(n) = \lim_{n\to\infty}\mathbf{P}^n\pi(0) \tag{37}$$

where $\pi = [\pi_1,\ldots,\pi_4]^T$ is the stationary distribution vector and π_i for $i \in \{1,2,3,4\}$ is the stationary probability of being in the i-th state and $\pi(0)$ is the probability distribution at the beginning of spectrum sensing $(n=0)$. The limit in (37) is solved by solving the following two equations:

$$\mathbf{P}\times\pi = \pi, \tag{38}$$

$$\pi_1+\pi_2+\pi_3+\pi_4 = 1. \tag{39}$$

Finally, the probability of miss detection and probability of false alarm corresponding to the dynamic BSS-based spectrum sensing scenario is:

$$P_m^{\text{dynamic}} = \frac{P\{\mathrm{H}_0^{CN},\mathrm{H}_1^{PU}\}}{P\{\mathrm{H}_1\}} = \frac{\pi_3}{P\{\mathrm{H}_1\}}, \tag{40}$$

$$P_f^{\text{dynamic}} = \frac{P\{\mathrm{H}_1^{CN},\mathrm{H}_0^{PU}\}}{P\{\mathrm{H}_0\}} = \frac{\pi_1}{P\{\mathrm{H}_0\}}. \tag{41}$$

It should be noted that the calculated dynamic performance measures is the distinctive feature of the proposed spectrum sensing method. Moreover, the performance of the proposed spectrum sensing method also depends on the behavior of the PU activity. In fact, if the real state of the PU (H_0^{PN} or H_1^{PN}) in the current sensing frame is repeated with a high probability in the next sensing frame, then the performance of the BSS sensing will increase noticeably.

4. Simulation results

In this section we analyze the performance of the proposed BSS-based channel sensing algorithm through numerical analysis. We compare the results in terms of receiver operating characteristic (ROC) curves for different BSS methods, SNR values and also for different number SUs as channel sensors. We provide simulation results in both cases when the SU transmitter is off and on. Then, for different errors of synchronization between primary and secondary frames, we compare the proposed method performance with a conventional ED method. In all simulations the sensing frame length L is equal to 100.

In **Fig. 5**, we have depicted the ROC diagram obtained by using different BSS-based spectrum sensing techniques for the case where the SNR is equal to 5 dB and the number of SUs is equal to 10. It is also assumed that the SUs are not in operation during spectrum sensing. We observe that in this scenario, the source separator based on comfac and Kurtosis outperform other competitive methods. Similar plots are depicted in **Fig. 6** for the case where the SU is in operation during spectrum sensing. Note that this feature is the main advantage of

BSS-based spectrum sensing compared to conventional methods since it allows simultaneous transmission and sensing for the SU. For comparison, we have also provided the sensing result obtained with a classical ED method, in the situation where the CR transmitter is ON. In this scenario, we observe that the Kurtosis signal separator outperforms ED and BSS-based all competitive methods significantly.

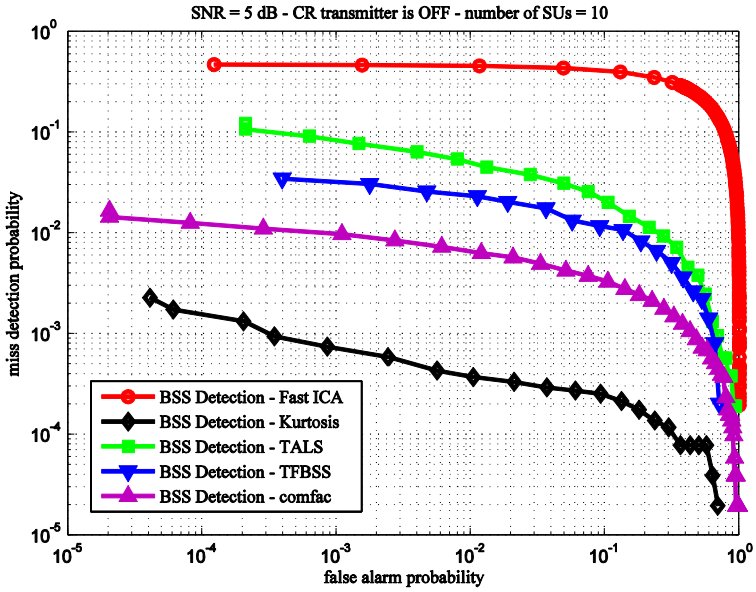

Fig. 5. The miss-detection probability versus the false-alarm probability for the comparison between different BSS-based spectrum sensing; the sensing SNR=5 dB, SUs number=10, CR Transmitter is OFF during spectrum sensing.

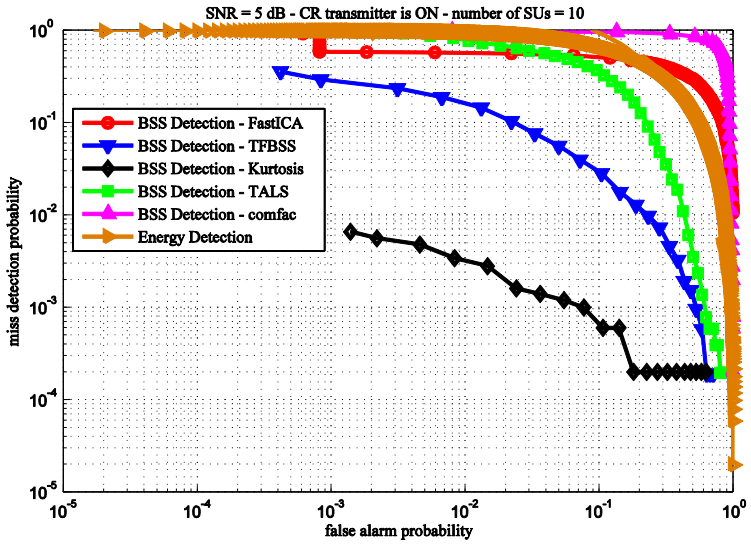

Fig. 6. The miss-detection probability versus the false-alarm probability for the comparison between different BSS-based spectrum sensing; the sensing SNR=5 dB, SUs number=10, CR Transmitter is ON during spectrum sensing.

In order to analyze the impact of sensing SNR on the performance of the proposed channel sensing method, we have shown in **Fig. 7**, different ROC diagrams for a sensing SNR value of 10 dB when the cognitive transmitter is active during spectrum sensing and when the number of SUs is equal to 10. Again, we can see that the proposed Kurtosis based method outperforms other BSS-based methods.

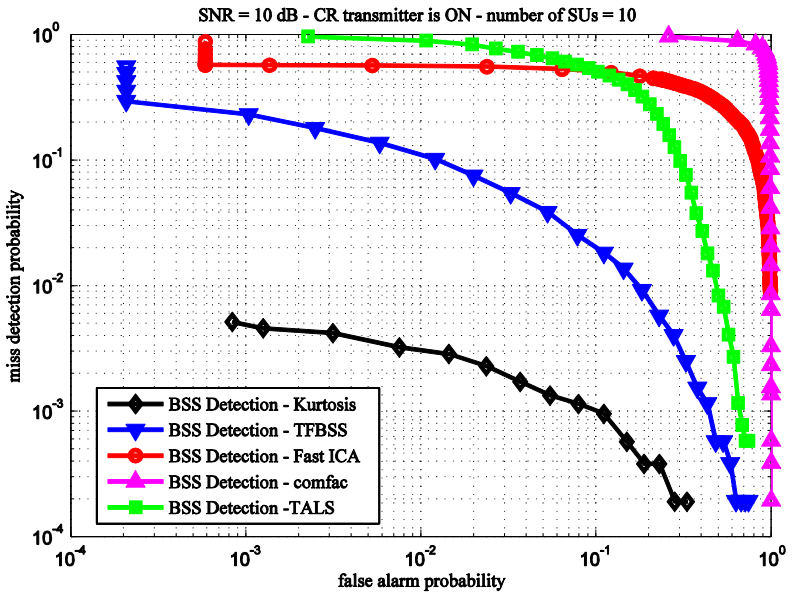

Fig. 7. The miss-detection probability versus the false-alarm probability for the comparison between different BSS-based spectrum sensing; the sensing SNR=10 dB, SUs number=10, CR Transmitter is ON during spectrum sensing.

As observed in previous simulation results, the main advantage of our proposed BSS-based spectrum sensing is when the SU is allowed to communicate with its base station during spectrum sensing. Obviously, this features leads to an increase of the overall throughput that can be characterized by smaller false alarm probability. Figure 8, compares the false alarm probability versus the number of SUs for different BSS-based spectrum sensing methods. We observe that the Kurtosis method provides the lowest false alarm probability (i.e., the highest throughput) compared to other competitive methods. Moreover, we observe that the false alarm probability decreases when the number of SUs increases. This observation is due to the fact that the accuracy of spectrum sensing is increased when a larger number of SU are involved in the spectrum sensing process.

In **Fig. 8**, we have plotted the probability of false alarm (for a fix probability of miss detection) versus the number of secondary users for different BSS-based spectrum sensing methods. This result lets us to compare the adequacy of each method in terms of secondary throughput, because lower false alarm means a larger throughput for the secondary network. We observe that the Kurtosis based method provides the lower probability of false alarm (equivalently, the larger secondary throughput) for a given number of SUs.

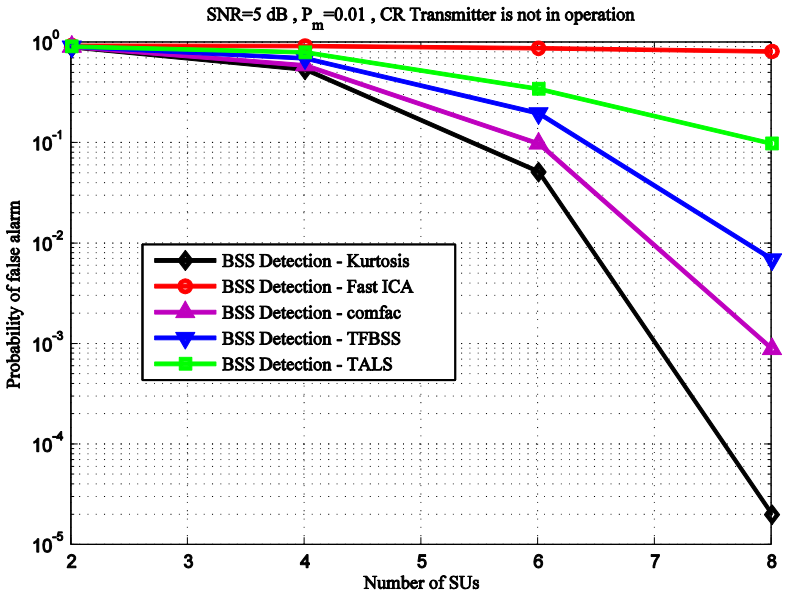

Fig. 8. Probability of false alarm versus the number of SUs at fixed probability of miss detection for different BSS-based spectrum sensing methods, the CR is assumed to be OFF during spectrum sensing.

In **Fig. 9**, we have set the probability of miss detection to 0.01 and analyze the probability of false alarm for different values of error in synchronization. For instance, a synchronization error of 50% means that the secondary has assumed that the middle of the primary frame is the beginning of the frame. We observe that the family of BSS-based spectrum sensing are not senstitive to frame synchronization errors while the conventional ED spectrum sensing is very senstive. For more SUs, the performance of both BSS-based spectrum sensing and the ED spectrum sensing would increase. However, the proposed BSS-based spectrum sensing is not sensitive to synchronization errors and therefore, yielding a better performance for errors in synchronizations.

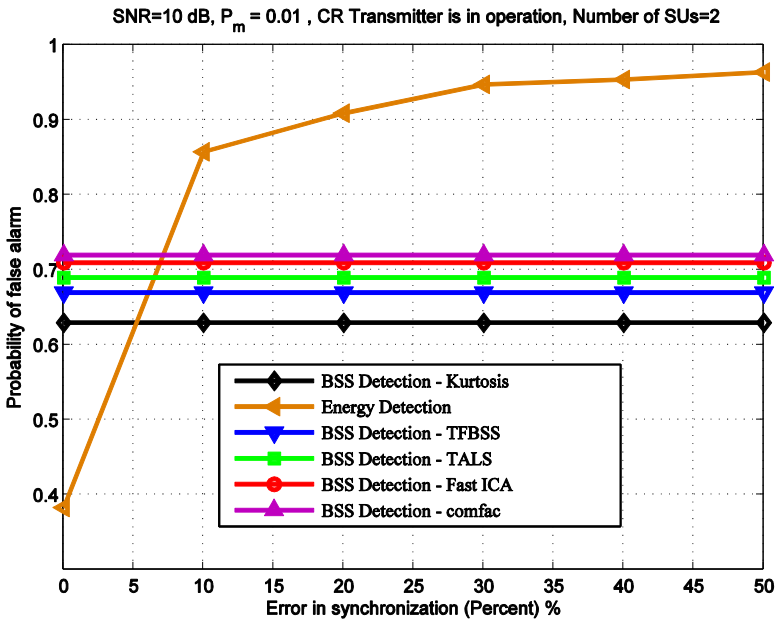

Fig. 9. False alarm probability versus error in synchronization. Comparison between conventional cooperative ED with 2 SUs and different BSS based methods.

In order to analyze the performance of the BSS-based spectrum sensing in the dynamic mode, we have shown in **Fig. 10**, different ROC diagrams for the proposed BSS-based method (Kurtosis based). The sensing SNR value is equal to 5 dB and the cognitive transmitter switches dynamically to ON/OFF states. The ROC diagrams are plotted for different ratios of sensing frame to the PU frame which is equal to $\varepsilon = 1/M$. It can be seen that the performance of the dynamic spectrum sensing is better for smaller values of parameter ε. Note that in this diagram, the sensing frame length is fixed and equal to $L = 100$, and the PU data frame length is assumed variable.

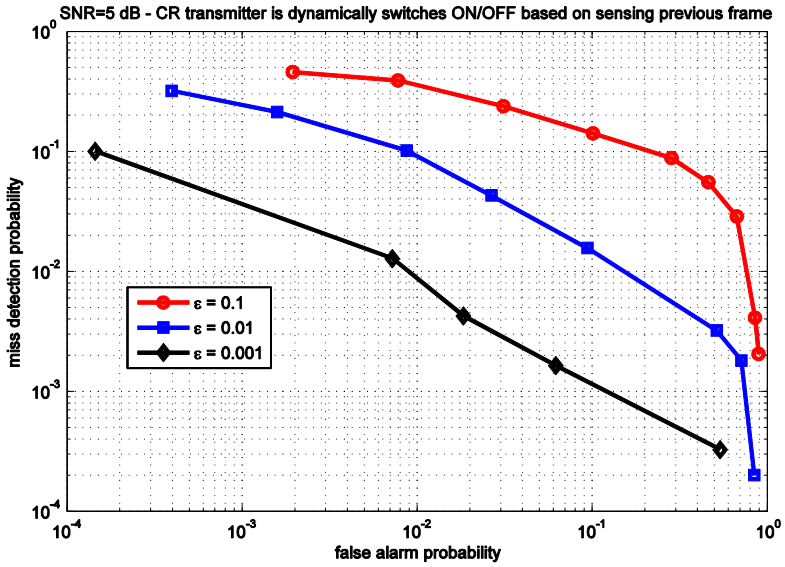

Fig. 10. The miss-detection probability versus the false-alarm probability for the comparison between different ratio of sensing frame to PU data frame. ε is the ratio of sensing frame to PU data frame.

5. Conclusion

In this paper, we proposed a BSS-based algorithm for spectrum sensing in CR systems. The proposed method uses BSS to recover two assumed original signals and then the properties of the recovered signals are determined in order to recognize and separate each initial source. Then, the decision about the presence or absence of the PU signal is made accordingly. We showed that the advantage of the proposed method is that the secondary sensing frame does not need to be synchronized with the primary data frame. The other main advantage of our method is that the secondary user can continue its transmission during spectrum sensing. In other words, the proposed method increases the secondary throughput compared to conventional methods such as ED that force the secondary to be inactive during spectrum sensing. We compared different type of BSS techniques and showed that BSS based on Kurtosis maximization outperforms other methods. It was also seen that performance improvement is more important when a larger number of SU is involved for spectrum sensing.

References

[1] Haykin, S. "Cognitive radio: brain-empowered wireless communications," *IEEE Journal on Selected Areas in Communications*, 23(2):201-220, 2005. Article (CrossRef Link).

[2] Ghasemi, Amir and Sousa, Elvino S. "Opportunistic Spectrum Access in Fading Channels Through Collaborative Sensing," *Journal of Communications*, 2(2):71-82, 2007. Article (CrossRef Link)

[3] Sun, Chunhua and Zhang, Wei and Ben Letaief, Khaled. "Cooperative Spectrum Sensing for Cognitive Radios under Bandwidth Constraints," *2007 IEEE Wireless Communications and Networking Conference (WCNC)*, pages 1--5, 2007. IEEE. Article (CrossRef Link)

[4] Khajavi, Navid Tafaghodi and Sadough, Seyed Mohammad-sajad. "Improved Spectrum Sensing and Achieved Throughputs in Cognitive Radio Networks," N*etwork*, 2010. Article (CrossRef Link)

[5] H. Sun, D. Laurenson, Cheng-Xiang Wang, "Computationally Tractable Model of Energy Detection Performance over Slow Fading Channels," *IEEE Communications Letters*, vol.14, no.10, pp.924-926, October 2010. Article (CrossRef Link)

[6] H. Sun, A. Nallanathan, J. Jiang and C.-X. Wang, ``Cooperative Spectrum Sensing with Diversity Reception in Cognitive Radios," in *Proc. IEEE ChinaCom'11*, Harbin, China, pp. 216-220, August 2011. Article (CrossRef Link)

[7] Yucek, Tevfik and Arslan, Huseyin. "A survey of spectrum sensing algorithms for cognitive radio applications," *IEEE Communications Surveys & Tutorials*, 11(1):116-130, 2009. Article (CrossRef Link)

[8] S. Choi, A.Cichocki, H. M. Park, S. Y. Lee. "Blind source separation and independent component analysis: A Review," *Neural Information Processing*, 6(1), 2005. Article (CrossRef Link)

[9] Lee, Chia-han and Wolf, Wayne. "Blind Signal Separation for Cognitive Radio," *Journal of Signal Processing Systems*, 63(1):67-81, 2009.

[10] Liu, Xin and Tan, Xuezhi and Anghuwo, Anna Auguste. "Spectrum Detection Of Cognitive Radio Based On Blind Signal Separation," *IEEE Youth Conference on Information, Computing and Telecommunication*, pages 166--169, 2009.

[11] Liu, Xin and Tan, Xuezhi and Anghuwo, Anna Auguste. "Spectrum Detection Of Cognitive Radio Based On Blind Signal Separation," *IEEE Youth Conference on Information, Computing and Telecommunication*, pages 166--169, 2009.

[12] Zheng, Yi and Xie, Xianzhong and Yang, Lili. "Cooperative spectrum sensing based on blind source separation for cognitive radio," in *Proc. of First International Conference on Future Information Networks (ICFIN)*, pages 398--402, 2009. IEEE.

[13] Khajavi, Navid Tafaghodi and Sadeghi, Siavash and Sadough, Seyed Mohammad-sajad. "An Improved Blind Spectrum Sensing Technique for Cognitive Radio Systems," in *Proc. of 5th International Symposium on Telecommunications (IST)*, number 4290, pages 13--17, 2010.

[14] N. Tafaghodi Khajavi, S. Sadeghi Ivrigh, S.M.S. Sadough. "A Novel Framework for Spectrum Sensing in Cognitive Radio Networks." *IEICE TRANSACTIONS on Communications*, E94-B(9):2600--2609, 2011.

[15] Sadeghi Ivrigh, Siavash and Sadough, Seyed Mohammad-sajad and Ghorashi, Seyed Ali. "A Blind Source Separation Technique for Spectrum Sensing in Cognitive Radio Networks Based on Kurtosis Metric," in *Proc. of International eConference on Computer and Knowledge Engineering (ICCKE)*, pages 327--331, 2011.

[16] Li, Xi-lin and AdalÄ ±, Tülay. "Complex Independent Component Analysis by Entropy Bound Minimization," *IEEE Transactions on Circuits and Systems I: Regular Papers*, 57(7):1417-1430, 2010.

[17] Papadias, Constantinos B. "Globally Convergent Blind Source Separation Based on a Multiuser Kurtosis Maximization Criterion," *IEEE Transactions on Signal Processing*, 48(12):3508-3519, 2000.

[18] R. Bro, N. Sidiropoulos, and G. B. Giannakis. "A Fast Least Squares Algorithm for Separating Trilinear Mixtures," *in Proc. of ICA99 Int. Workshop on Independent Component Analysis for Blind Signal Separation*, pages 289-294, 1999.

[19] Nicholas D. Sidiropoulos, Georgios B. Giannakis and Rasmus Bro. "Blind PARAFAC Receivers for DS-CDMA Systems," *IEEE TRANSACTIONS ON SIGNAL PROCESSING*, 48(3):810--823, 2000.

[20] Cédric Févotte and Christian Doncarli. "Two Contributions to Blind Source Separation Using Time–Frequency Distributions," *IEEE SIGNAL PROCESSING LETTERS*, 11(3):386--389, 2004.

[21] A. Hyvarinen, J.Karhunen, E.Oja. "Independent Component Analysis.," *John Wiley & Sons*, 2001.

[22] A. D. Allen. "Probability, Statistics and Queueing Theory," *Academic Press New York.*